Corrosion Behaviors of Aluminum Following a Loss of Coolant Accident

Undergraduate Honors Thesis

Presented in Partial Fulfillment of the Requirements for Graduation with Distinction in the Department of Mechanical Engineering of The Ohio State University

By

Amanda Sue Wen Leong

Mechanical Engineering

The Ohio State University

2017

Thesis Committee:

Jinsuo Zhang, Advisor

Annie Abell

Abstract

Aluminum (Al) corrosion in the containment of nuclear reactor has detrimental effects on the performance of emergency-core–cooling system (ECCS). In a loss-of-coolant accident (LOCA), the ECCS is initiated to shut down the operation of a nuclear power plant safely. The cooling alkaline solution flowing through the ECCS has a high concentration of boric acid, which has been suggested to be corrosive to Al alloy. Precipitations caused by Al corrosion potentially obstructs the sump screens while the solution is re-circulated in the nuclear core through ECCS. This study aims to understand the release and corrosion behaviors of Al alloy exposed to the boron-containing alkaline solution.

The corrosion rate of Al was determined through obtaining the mass of Al released into the solution as well as the formation of scale on the Al sample. The test conditions were referenced for the prior literature reviews [1] [2] [3] [4] as well as the actual design of PWR. To explore further into the effect of Al corrosion towards the ECCS, the effects of temperature, pH and submersion time of Al which exposed to the borate buffer solution have been studied. Experiments were undertaken in a shaker table equipment which simulates the conditions of Al exposure to the containment sump following a LOCA.

Results have shown that at a higher temperature, the corrosion rate of Al was significantly higher. Across a period of submersion time of Al in solution, the corrosion rate of Al decreased drastically. Al corrosion rate is higher at higher pH and temperature. At 85 ℃, the dissolved Al re-deposit on the sample surface which makes less Al dissolved in solution.

Acknowledgements

First, I would like to express my utmost gratitude to my advisor Dr. Jinsuo Zhang. He has been my pillar of support throughout this whole research process. I appreciate his kindness and effort in guiding me in this research. I would also like to thank him for his willingness to teach and his care for the safety of the students working in the lab. He is always open to discuss questions and to suggestions. He has been a great support academically as well as financially, and this research will not be successful without his help.

Secondly, I would like to thank Dr. Yi Xie for her willingness to spend time with me and guiding me through the process of writing this thesis. Her input is always very helpful and truly appreciate her sincerity in helping students.

I also want to thank Dr. Shaoqiang Guo. He is always generous in time by patiently discussing issues with us. He is never shy with his knowledge and always willing to teach anytime you ask him a question.

I would also like to take this opportunity to thank Dr. Janet Levitt and Mark Macali, for their commitment towards this research project. Their contributions are vital for the success of this research project.

I would also like to thank Dr. Robert Siston for his guidance throughout this past year and his help on teaching me the best practices on research presentation. He is very resourceful and is always happy to share his experience in research with his students.

I would also like to thank Dr. Annie Abell for being one of the committee for my defense. Lastly, I want to thank God, without Him, none of this would have happened. I thank Him for His faithfulness and love.

Table of Contents

List of Figures

List of Tables

Chapter 1: Introduction

Operational nuclear power plant adheres to the environmental safety guidelines which ensure the public prevented from radiation. A loss-of-coolant accident (LOCA) serves as a potential threat; this is a scenario in which coolant from the primary coolant loop suffers significant reduction due to a pipe break. During leaking, primary coolant coming out from the pipe is leaving at high temperature and high pressure, thus, the insulation and other debris may fall into the containment sump and would be exposed to pressurized water. During a LOCA, the nuclear power plant will activate an ECCS to assist in core heat removal by recirculating the coolant from the containment sump as shown in Figure 1.

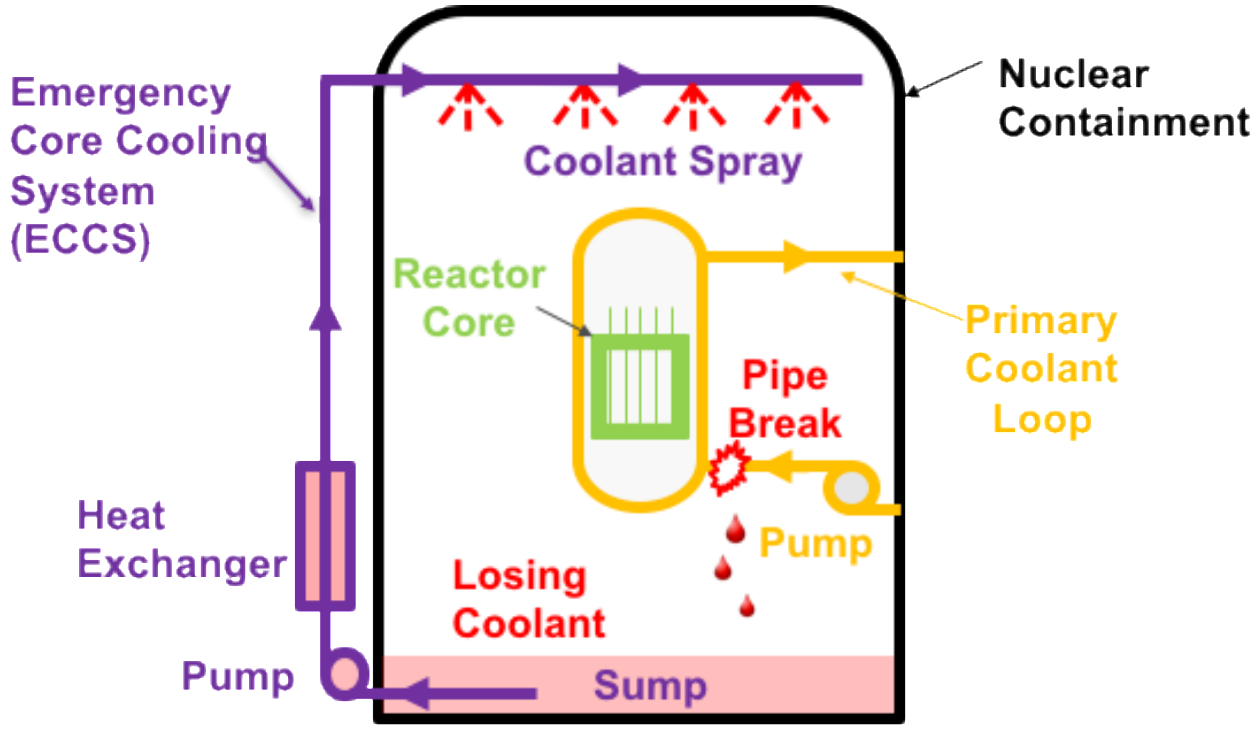

Figure 1: Illustration of ECCS system during a LOCA in a nuclear power plant.

The ECCS system components are protected with debris strainers are assembled at the outlet of containment sump to prevent debris from entering into the ECCS suction lines. Loose debris in LOCA will accumulate on the strainers in the containment sump. Results have shown that the accumulation of debris may form a bed at the sump screen which impedes the recirculating flow of the ECCS system [5]. ECCS suction systems are susceptible to fail when a lot of materials (include metals and debris) release in the corrosive coolant. This is because the coolant ejected into the nuclear containment through the pipe break from the primary system will increase the temperature and pressure within the containment. The coolant made of up high concentration of boron and as the corrosive coolant comes in contact with the materials in the containment, it will erode the materials, this includes Al as it serves as one of the main components in the containment. Materials were releasing into the corrosive coolant and form precipitations due to the changes of temperature in the large containment. These precipitates will fall into the containment sump. This accumulation of debris tends to form a layer of obstruction before the pump strainer thus loss of net positive suction head across the strainer [3]. On top of that, the submerged metallic components are still subjected to corrosion over a long period even after the ECCS system stops working.

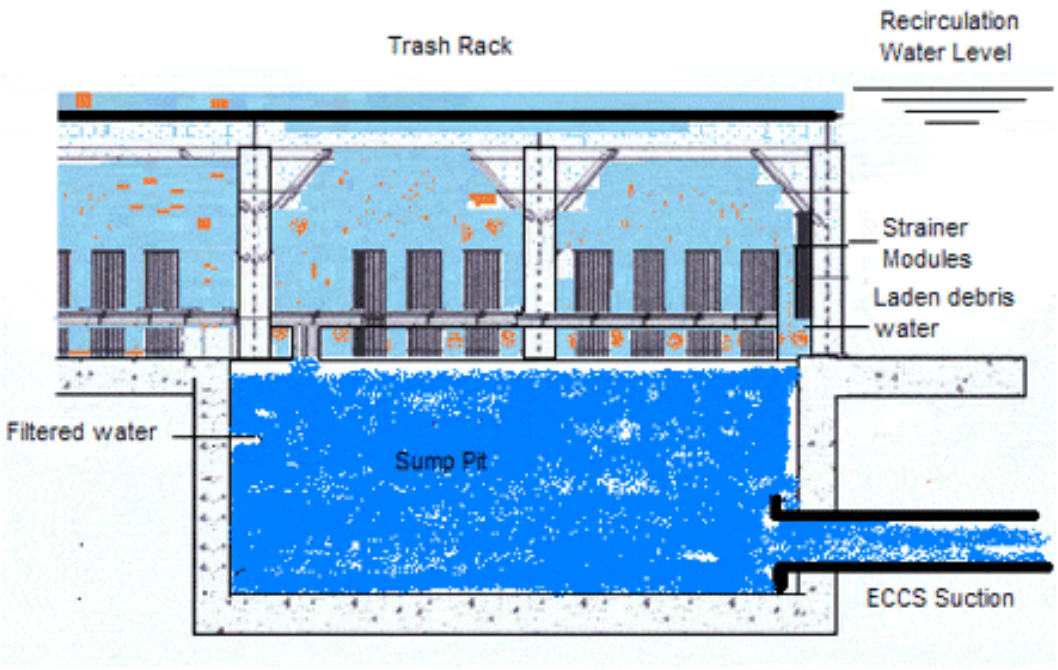

Figure 2: Illustration of containment sump [1].

Figure 2 is a typical containment sump design, showing the arrangement of strainers above the sump pit where all the coolant in the nuclear containment accumulates. Coolant would have to flow through levels of strainer modules before it reaches the sump pit. With a particulate presence in the coolant, this increases the difficulty of coolant to flow through the sump strainer. This can be compared to a filtration system, where the coolant is purified through a series of rocks, however, in this case, the result of this is a reduction of coolant in the sump pit.

If the situation persists, this could lead to a nuclear core meltdown thus becoming a serious hazard to the public. Therefore, it is our responsibility to reduce the chances of this disaster to occur. To resolve this issue, Nuclear Regulatory Commission (NRC) issued a generic-safety-issue (i.e. GSI-191) to all licensees of operating reactors, applicants for operating licensees and holders of construction permits in 1985 [2].

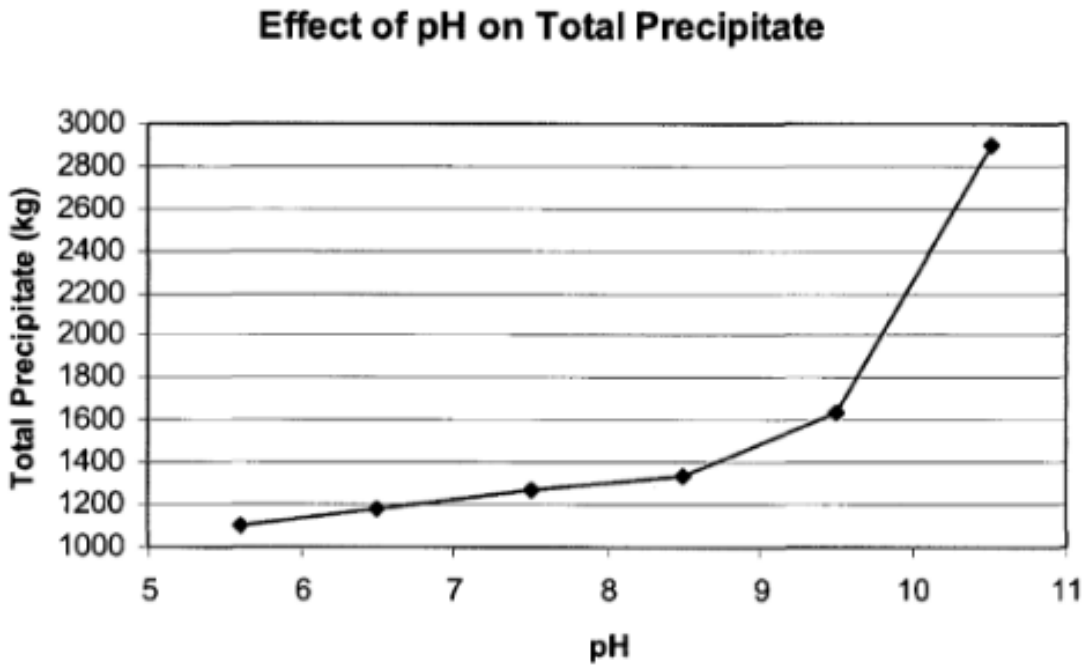

Figure 3: Effect of pH on total precipitate mass [5].

According to the report from Westinghouse, results have shown that with the increase of pH of solution results in an increase in the total amount of precipitates. It has also been reported that the corrosion of Al during the spray phase post-LOCA is the main contributor to the precipitates increases at high pH values. The amount of total precipitates is also sensitive to temperature change as described in the report from Westinghouse, where the change was about 20 %. However, the effect was mainly a result of an increase of Al corrosion with temperature [5]. According to the previous literature review, Al corrosion increases rapidly as pH increases above 6 [6] [7] [8] [9]. Chen et al. attributed that solution conditions following a LOCA increase the corrosion rate of Al dramatically [10].

Therefore, the objective of this project is to study how the Al saturation condition of buffer solution across a period of time. The primary focus of this research project is on the change of saturation state of Al into the borate buffer solution with varying temperature and pH of the

solution. The tests were simulated at three different pH levels. Since LOCA occurs when there's a pipe break, the temperature and pressure of the coolant leave the pipe at various intensity levels. This affects the pH of the coolant leaving the pipe based on the break size of the pipe. Therefore, it was necessary to understand the saturation condition of the Al-based on simulation of different pipe breaks.

Chapter 2: Brief review of Al corrosion in boron-containing alkaline solution

2.1 Chemical composition of Al ions and corrosion mechanism

Al readily forms an oxide layer on its surface when exposed to air [10]. This oxide layer protects the substrate Al and controls the corrosion rate of the material depending on the thickness of the oxide layer. However, Al reacts differently in water; the oxide layer disintegrates [11]. The degree of corrosion also depends on the relative rates of oxide layer growth and breakdown [11]. Previous research has claimed that the dominant mechanism of pure Al corrosion is mainly determined by the anodic reaction of Al in alkaline solution [12] [7]. The mechanism involves formation and dissolution of an oxide layer continuously. The following is an equation that depicts the mechanism [10].

$$2Al + 6H_20 + 2OH^- \rightarrow 3H_2 + 2Al(OH)_4^- \qquad \textit{Equation 1}$$

The pH, temperature, fluid velocity, surface to volume ratio of the solution, duration of submersion and the presence of anions affects the corrosion rate [10]. The experiments have been performed to specifically study how pH temperature and duration of submersion affects the corrosion of Al. The boric acid composition in the solution reaction towards Al corrosion is strongly influenced by temperature. Some results have shown that Al corrosion rapidly increase above pH 6, and the corrosion rate decreases as the Al submersion time increases [6].

As the dissolution reaction of Al determines the Al solubility in alkaline solution while the releasing of Al into the solution is represented by the following equation [13].

$$Al_{ej} + 3OH^- \rightarrow Al(OH)_3 + 3e \qquad \textit{Equation 2}$$

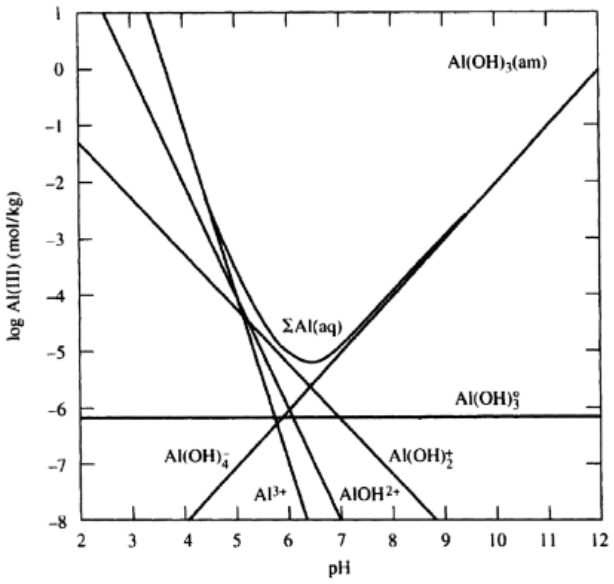

Figure 4: Solubility of an amorphous $Al(OH)_3$ as a function of pH at 25 ℃, lines indicate the solubility of concentrations of Al^{3+} *[14]*.

In Figure *4*, the equilibrium solubility of different forms of Al ions and the correcting total Al concentration in the solution at different pH values was shown [14]. Based on the plot, $Al(OH)_4^-$ is the only stable form which dissolves in the alkaline solution and its dissolubility increases with the increase of pH. Based on Figure *4*, the solubility of $Al(OH)_4^-$ increases linearly as the pH increases. However from the figure, other Al ions such as Al^{3+}, $AlOH^{2+}$, and $Al(OH)_2^+$ were not as stable at 25 ℃ [15].

According to Zhang et al., there are two processes that are competing between each other for Al corrosion [15]. This first is the direct dissolution of Al metal while the second is the chemical formation of Al hydroxide films. The first process is very reactive as a result it increases the corrosion rate of Al However, as the elapsed time of the exposure of Al to solution increases, the second process takes place, and the film continuously builds up on the surface of the Al Thus, the corrosion rate of Al significantly reduces as this protective layer forms [15]. Since $Al(OH)_4^-$ is the

main form of ions that are stable in alkaline solution, which corresponds to chemical equation

R

E

F

_

R

e

f

4

7

7

0

2.2 Characteristics of boron in the solution

3

In support of the GSI-191, understanding the behavior of aluminum in the coolant used in

3

the ECCS is vital. Boric acid used as a pH buffer solution can play a role in controlling the

3

reactivity as a coolant in the pressurized-water-reactor (PWR). As reactivity in a nuclear core is

1

an important control, this reaffirms the importance of understanding the interaction of aluminum

8

with boron, especially in post-LOCA. Precipitation may occur when boron interacts with Al in a PWR; this will reduce the efficiency of the ECCS system. Zhang et al. reported that boron was

\

found on the hydroxide solid and exist on the solid as absorbed ions [15]. Beyrouty et al. found

h

that the boron adsorption inhibits the crystallization on the surface of Al [17]. The presence of boron is due to the boric acid present in the reactor core used to balance out the pH of the

\

*

primary coolant. In an incident of a LOCA, the pH of the coolant is approximately at 10 when the ECCS is activated [15]. According to Baes et al., at high concentration and between pH 6 to pH 11, highly water soluble poly-borate ions are formed [18]. Apart from that, the adsorption of boron onto aluminum is also highly influenced by temperature. Previous research has shown that higher temperatures result in a lower boron absorption [19]. According to Figure 5, the absorption of boron at 25 ℃ if affected by the pH. According to Su C. et al., boron adsorption is bell-shaped, and results have shown that there is an increase in boron adsorption from pH 3 to 6 and peaks at pH 6.5 to 8.5, and decrease from pH 8.5 to 12 [19]. This is also due to the un-dissociated boric acid at pH values lower than 7, while at higher pH values, $B(OH)_4^-$ ions dominantly exist while there is still a possibility that $B_3O_3(OH)_4^-$, $B_4O_6(OH)_4^-$, and $B_5O_6(OH)_4^-$ may form [15] [20].

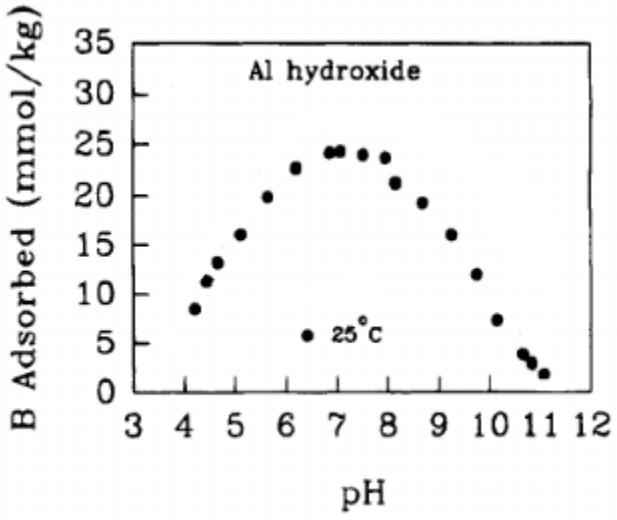

Figure 5: Boron Adsorption as a function of pH on Al at 25 ℃ *[19]*.

The pH of the solution in this experiment lies within the range from pH 7.5 to pH 8.2 which is within the peak boron adsorption rate. Boron adsorption occurs through compact

formation with the hydroxyl groups on the surface of the Al [15]. Since the range of pH tested in this experiment is within the peak range as reported by Su. C et al., therefore the B adsorbed to the Al should remain constant. Chen et al. stated that even with variability in the measured corrosion rates from different researchers and with different methods the corrosion rate of Al in solution conditions following a LOCA is 1–2 orders of magnitude higher than at similar pH and temperature when there is no borate in solution. As a result, with higher temperature, aluminum corrosion rate increases. Similarly, the higher the concentration of boron, the higher the solubility of Al [20].

Chapter 3: Design of System

A shaker table system (Model 10000-1 VWR) was developed to simulate the conditions of LOCA in a nuclear containment. The condition of flow in the nuclear containment is simulated using the shaker table, using a constant translation platform in the XY direction. The system has the ability to house 25 test at the same time, however with a limitation of similar temperature test environment. The temperature of the experimental setup is circulated based on temperature regulator (Model FTE10DPC Techne). The volume of water in the reservoir was maintained at a higher temperature to account for heat loss. The water heated by the temperature regulator remains isolated from the water in the test container. Black polyethylene insulations shown in the figure were used to wrap around the testing equipment to reduce heat loss to the surroundings. Both the reservoir and the testing container are made up of polyethylene that is impact resistant.

Figure 6: Experimental components in the shaker table system (1. heat circulating, 2. reservoir, 3. heat bath, 4. shaker table, 5. circulating pipe and 6. insulation).

Based on the schematic of the experimental setup in Figure 7, the circular slots represent the location of individual test bottles are placed. The placement of the bottles is usually evenly distributed over the 25 slots if not all of them will be filled. On the other hand, the temperature is maintained by the water in the reservoir controlled by a water temperature regulator. Heated water will flow into the heating coil placed on the bottom of the test container to heat up the water in the test container, while the temperature on the reservoir regulator is preset to a higher temperature to account for heat loss. The motion of flow in the nuclear containment was then simulated by using the shaker table revolving system.

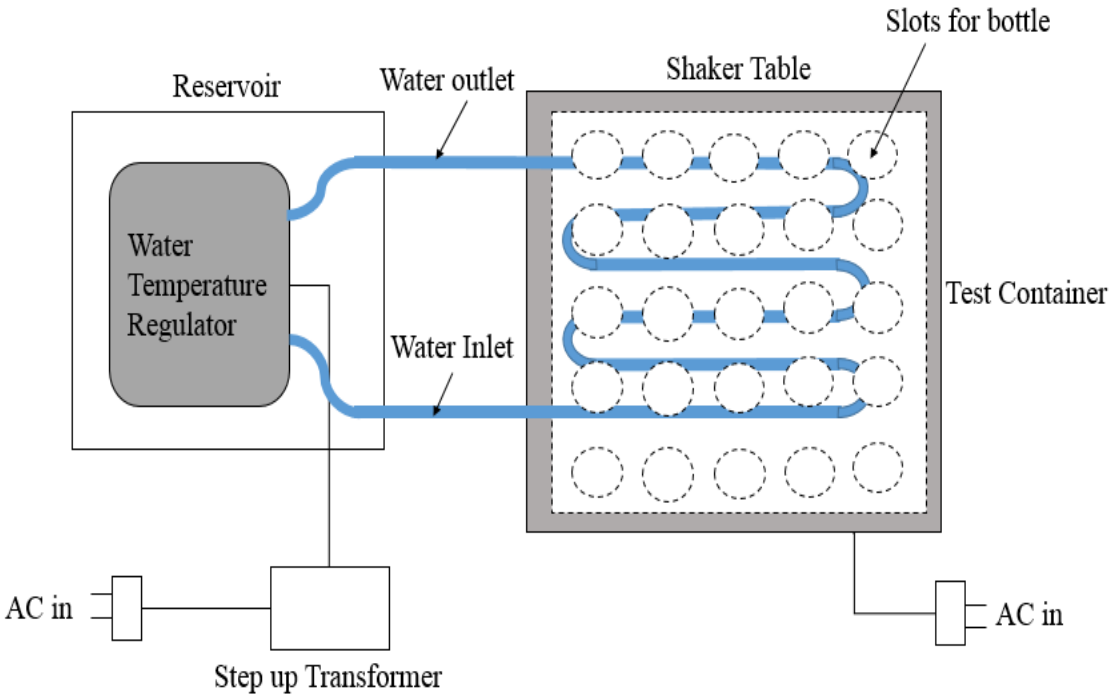

Figure 7: Top view schematic diagram of shaker table system.

Based on the road map in Figure 8, one can follow the procedure to accurately startup the system.

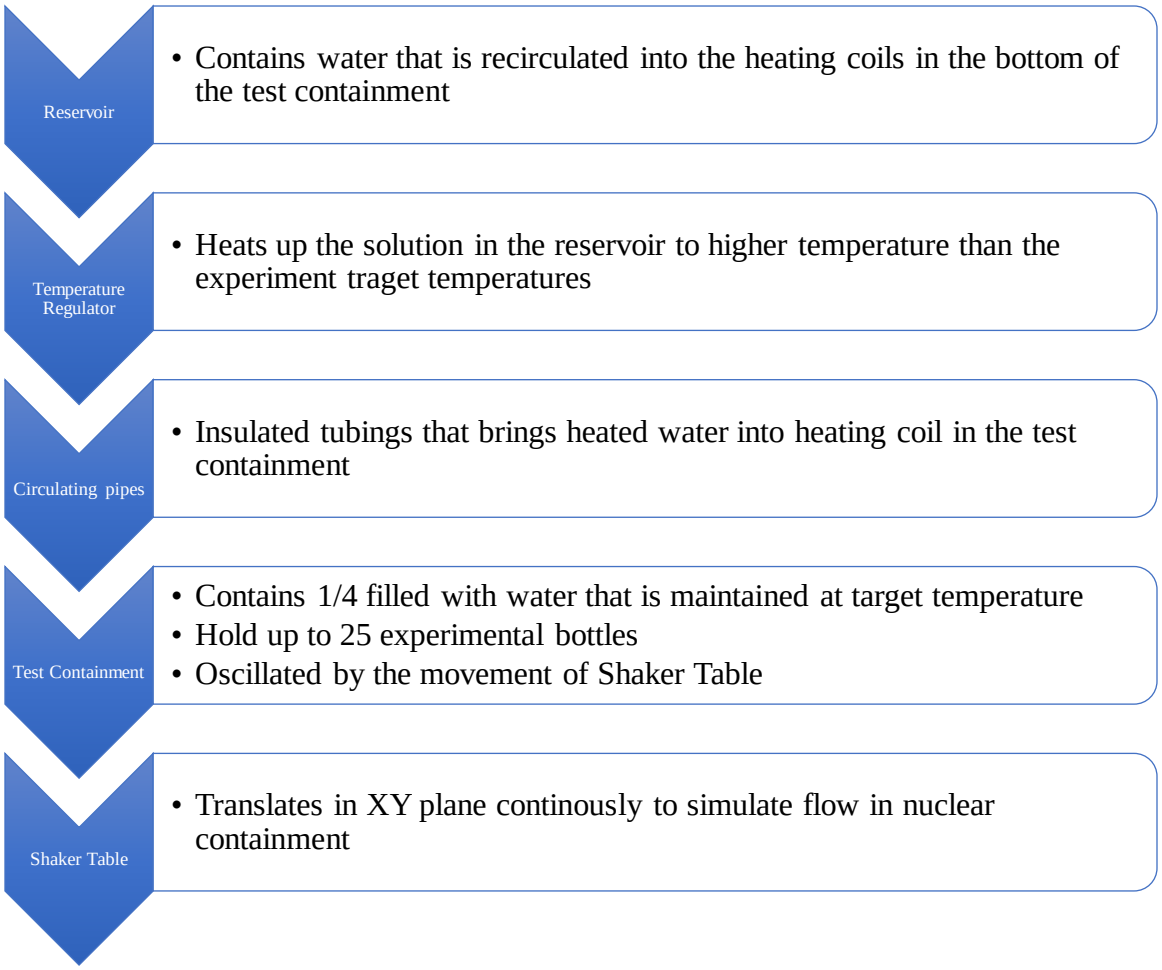

Figure 8: Road map of shaker table design

Chapter 4: Experimental Methodology

4.1 Material and Solution

Al sheets of 1100 alloy were used to fabricate specimen of 43 mm square and 1.6 mm thick with a 3 mm diameter hole at the top center of the specimen. The surface finish of the specimens was polished with a series of SiC papers from grits of 120 followed by 500 and 800. The desired surface area exposure of the specimen is $0.004\ \mathrm{m}^2$. The thickness of the specimens was within $\pm\ 0.1\ \mathrm{mm}$, while the width and length of the coupons were within $\pm\ 3\ \mathrm{mm}$. Even with the dimension variability, the surface area of the specimens exposed was kept within $\pm\ 0.0005\ \mathrm{m}^2$. The specimens were cleaned with distilled water and rinsed with ethanol. The dried and cleaned specimens were then kept in air for at least 24 hours before tests.

Each test containment is made up of 500ml of borated buffer solution. The buffer solutions were prepared based on the chemical compositions shown in Table 1. The respective amount of chemicals were dissolved in distilled water before the pH of the solution was measured at room temperature. The pH 8.2 borate buffer solution was prepared by adding approximately 0.85 ml of 15M NaOH into pH 7.5 borate buffer solution since both borate buffer solution has similar chemical Composition, the adding procedure ceased until target pH was reached at room temperature. Lab grade Boric acid, H_3BO_3 and Sodium Tetraborate, $Na_2B_4O_7 \cdot 10H_2O$ were measured using an analytical balance within± 0.0005g.

Table 1: Chemical compositions of borated buffer solution.

Chemical	pH		
	7.5	**7.7**	**8.2**
H_3BO_3 (g)	5.7534	5.7534	5.7534
$Na_2B_4O_7 \cdot 10H_2O$ (g)	1.6342	1.9398	1.6342
15 M NaOH solution (mL)	0	0	0.85 ± 0.15

4.2 Immersion Test

The borate buffer solutions were poured into 1 L HDPE wide-mouth bottles, which serves as individual test containers. All HDPE bottles were rinsed triple times and air dried to ensure that they are not exposed to external particulates. Prepared borate buffer solution bottles without specimens were placed in the equipment to allow the solution to stabilize at the target temperature for at least 12 hours. After the temperature of the medium stabilizes, specimens can be inserted into individual bottles which mark the start time of the test.

The specimens were hanged using nylon strings of 1.6 mm diameter. Specimens were inserted into the HDPE bottles with borated buffer solutions at the target temperature and sealed with wide mouth caps. All specimens were drooped into a position whereby it is fully submerged in the solution but still hanged freely without coming in contact with the walls of the bottle. Throughout the experimental period, the temperature of the test environment was maintained within ± 3 °C of target temperature. The temperature of the test environment was measured and verified with a NIST certified thermometer daily. External distilled water in the testing equipment was replenished daily to ensure that system remains in normal operation mode.

4.3 Inductively Coupled Plasma (ICP) Mass Spectrometry

ICP is an analytical approach used to determine elements. This technique gains general acceptance in various types of laboratories after it was introduced in 1983. ICP mass spectrometry is a combination of a high temperature inductively coupled plasma source with a mass spectrometer. The elements in the sample were converted from atoms into ions with the help of the ICP source than these separated ions are detected by the mass spectrometer [21].

ICP Mass Spectrometry was done on every test solution to obtain the releasing rate of Al Once the experiment was done, 30mL of buffer solution was removed from the bottle and stored in a HDPE container. To obtain the releasing rate of Al, the solution from every test was diluted individually. The dilution process was done by measuring the weight of the solution, nitric acid and distilled water needed. The ICP diluted solution was then placed into the mass spectrometry machine for analysis.

According to Musa et al., nitric acid readily attacks Al, therefore this disturbs the ability of Al to form Al oxide, thus preventing Al precipitation [22]. Therefore, using nitric acid in the ICP solution will keep the post-experiment Al ions in its form, and the actual amount of Al ions can be measured and accounted in the release rate.

4.4 Sample Descaling

The post-test samples were descaled following the ASTM G1-03 [23]. Descaling is an approach use to remove a layer of scale on the surface. Al is a material that actively forms a layer of oxide as it reacts readily with oxygen. Throughout the experiment, layers of Al hydroxide was found on all experimental coupons. Therefore, to obtain the actual weight of the Al sample, and to account for the total weight loss of Al after a test, the Al sample must be descaled. The process of

descaling includes utilizing acid to erode the layer that was formed on the Al sample after the test. To efficiently remove the scales, the Al samples are submerged in diluted acids under heated conditions for short intervals, multiple times [4]. Descaling continues until the change in weight is less than 0.005g. The actual weight of the aluminum can then be determined from this process.

Chapter 5: Results and discussion

The tests were performed based on the manipulation of temperature and pH of borate buffer solution over a period. The test time ranged from 4 hours to 30 days. Within the testing period, Al release and scale mass were obtained to calculate the final corrosion rate of Al The effects of both pH and temperature parameters were compared to Al releasing. The releasing rate of Al was calculated based on the Al concentration level saturated in the test solution. The Al concentration level in the test solution was also compared at different temperature and pH values. In the end, the corrosion rate of Al was obtained through Al releasing rate and descaling results. Dall et al. found that at high pH solutions, Al is extremely susceptible to corrosion, especially in the presence of sodium hydroxide and sodium tetraborate[10].

5.1 Effects of pH on Al releasing

Al releasing rate into the buffer solution based on ICP measurements decreased as the time of immersion test increased. All solution at pH 7.2, 7.7 and 8.2 showed a similar decreasing trend, with pH 8.2 having a higher releasing rate followed by pH 7.7 and pH 7.5. The dissolution of Al was significantly higher as observed at pH 8.2.

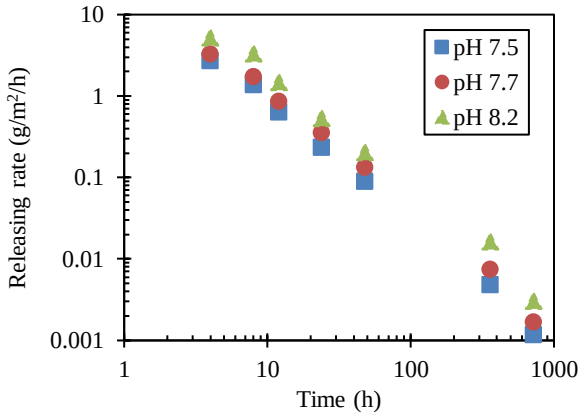

Figure 9: Releasing rate of Al at 85 °C.

The releasing rate of Al at 55 ℃ was lower than the releasing rate of Al by a factor of 10. **Error! Reference source not found.** shows that at 85 ℃ the difference of releasing rate of Al was much higher than the releasing rate of Al at pH 7.5 and 7.7 after a longer extended period of immersion test. At 55 ℃ under 10-hour immersion tests, the releasing rate of Al at pH 7.7 was lower in contrast with at 85 ℃.

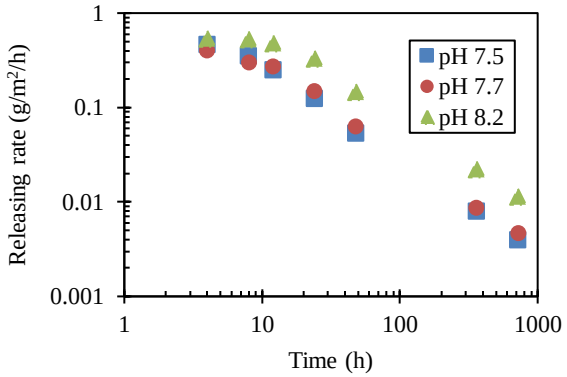

Figure 10: Releasing Rate of Al at 55 ℃.

At 25 ℃, the releasing rate of Al showed a similar trend as 55 ℃, whereby immersions test less than 10-hour has a lower releasing rate of Al at pH 7.7 than pH 7.5. As shown in Figure 11, at long immersion test time, the releasing rate of Al after 100 hours at pH 8.2 was significantly higher than pH 7.5 and 7.7.

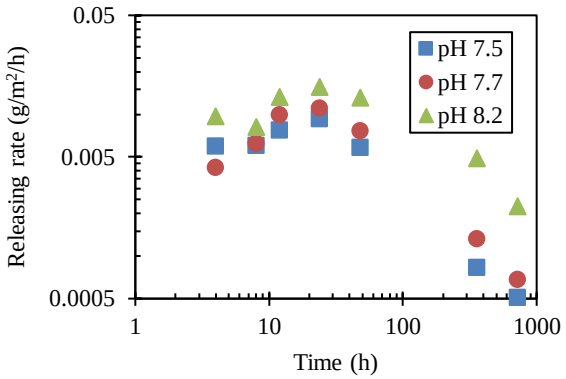

Figure 11: Releasing Rate of Al at 25 °C.

As shown in Figure 12, Al concentration is higher at the beginning of the experiment, as at high pH this is caused by the concentration of OH^- that encourages the dissolution of Al The Al concentration in solution decreases as the immersion test time increased. High pH value solution has shown to have a higher Al concentration in the solution. The Al concentration decreased exponentially during the first 48 hours. Al concentration in the solution stopped changing drastically after 48 hours in all 3 cases of pH values. At 720 hours, the Al concentration trends to a similar value. The releasing rate of Al in a pH 8.5 solution decreases after 20 days. It is possible that high OH^- with the Al surface layer increases the transportation rate of ions when the reaction rate is smaller as described by Chu et al. [16]. This significantly reduces the amount dissolution rate of Al when the layer of oxide is formed on the surface. Thus, stopping the production of $Al(OH)_4^-$ ions. This result is consistent with previous students that the dissolution of Al increases with the increase in pH.

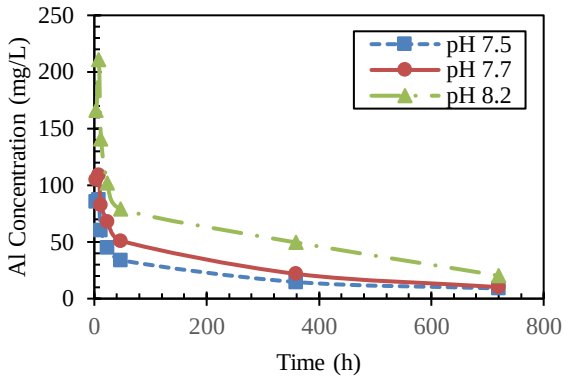

Figure 12: Al concentration over time at 85 °C.

At 55 °C, the trend of Al concentration over time has drastically different trend than at 85 °C. The Al concentration of pH 8.2 was higher than pH 7.5 & 7.7 by a factor of two. On the other hand, pH 7.5 and 7.7 Al concentrations were similar at 55 °C. As shown in Figure 13, Al concentration increases within the first ten hours and then the Al concentration remains the same with little increment. Bahn claims that up to 35% of the boron in the initial solution may have been adsorbed onto the Al as amorphous Al hydroxide precipitate [3]. Therefore, it may also be the reason why Al concentration in the initial testing period is high.

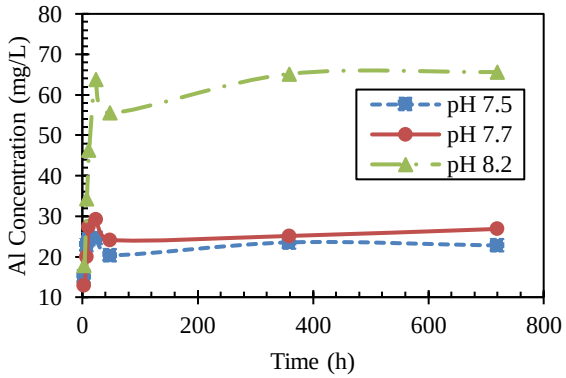

Figure 13: Al concentration over time at 55 °C.

At 25 ℃, the Al concentration for pH 8.2 continuously increased over time, while the Al concentration level converges after 48 hours for pH 7.5 and 7.7 solutions. Based on the following figure, the Al concentration in solution has drastic changes in first two days of post-LOCA.

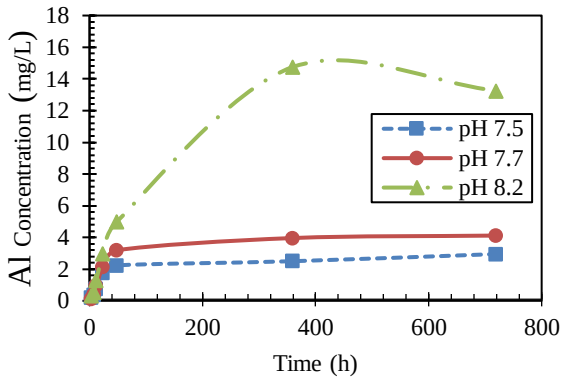

Figure 14: Al concentration over time at 25 ℃.

5.2 Effect of temperature on Al releasing

The trend of Al releasing rate tends to decrease over time. Results have shown that after 100 hours, the releasing rate of Al at 85 ℃ was lower than at 55 ℃ and this trend is similar across pH 7.5 to 8.2. One of the reasons for this phenomenon may be a result of a thick layer of formation of an Al oxide layer on the surface of the metal that serves as a protective layer. It has also been reported that the product of Al precipitation is amorphous. However, it will eventually be transformed into a stable crystalline structure. This crystalline structure is less soluble than the amorphous Al precipitation. The dissolution of Al into the alkaline solution as $Al(OH)_4^-$ reduces as the transport rate is faster than the reaction rate. This results in the reaction rate between the surfaces of the metal becoming a limiting factor. As a result, the crystalline form is less soluble than the amorphous structure; this causes the precipitate to not re-dissolve in crystalline form at a higher temperature. This transformation is still dependent on time temperature and solution chemistry [20].

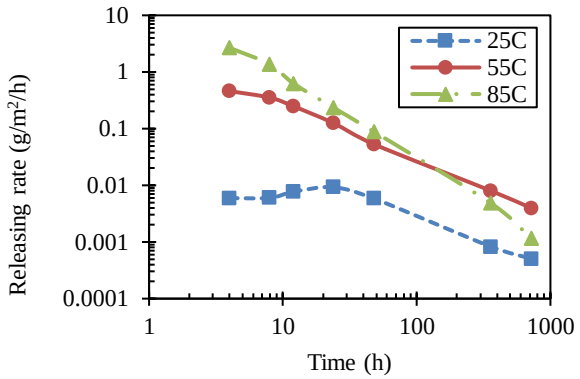

(a)

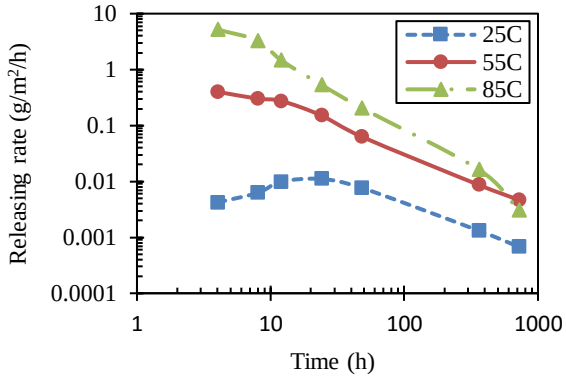

(b)

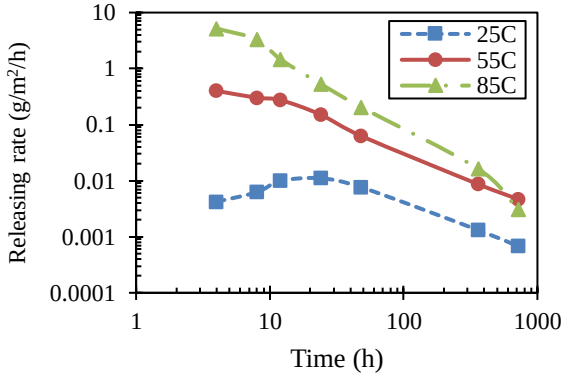

(c)

Figure 15: Releasing rate of Al over time of different borate buffer solution (a) pH 7.5 (b) pH 7.7 (c) pH 8.2

The following figures were made in relation to different temperature values. Results have shown that the corrosion rate change is the highest the first 12 hours of post-LOCA. The trend of

the curve slowly converges to a constant value after 48 hours. Similarly, the Al concentration at 55 ℃ was higher than 85 ℃ after 360 hours. From this, we can deduce that after 15 days the Al corrosion at 85℃ experienced significant reduction.

From Figure 16, the Al concentration plateaus after 48 hours at both 25 ℃ and 55 ℃ while at 85 ℃ the Al concentration level drastically decreases. The difference between the solutions is the presence of NaOH in the pH 8.2 solution. Approximately 1 ml of 15 M of NaOH solution were added into 500 ml of 7.5 pH test solution to obtain a pH 8.2 solution. Based on the results, we can deduce that the NaOH possibly inhibits the Al corrosion. The effect of this phenomenon takes place after the first 48 hours. As discussed before, initial Al precipitation is amorphous; this is also caused by the high concentration of anions known to inhibit the crystallization of Al at temperatures lower than 60 ℃ [3]. Previous studies have also shown that the crystallization of Al hydroxide film is depended on the degree of saturation regarding Al solubility in alkaline solution [24]. A significant amount of Al will not precipitate but will remain in the solution as dissolved form or possibly small sized particles which will not induce head loss around the debris bed on the sump strainer [3].

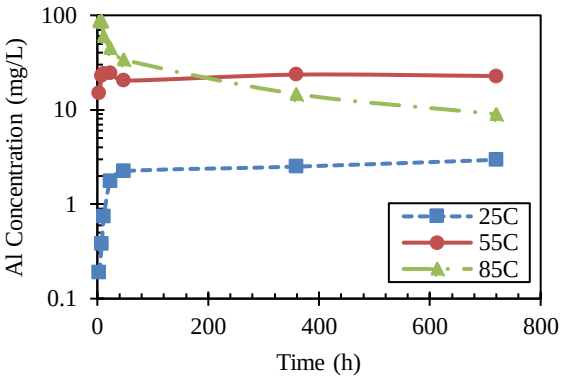

(a)

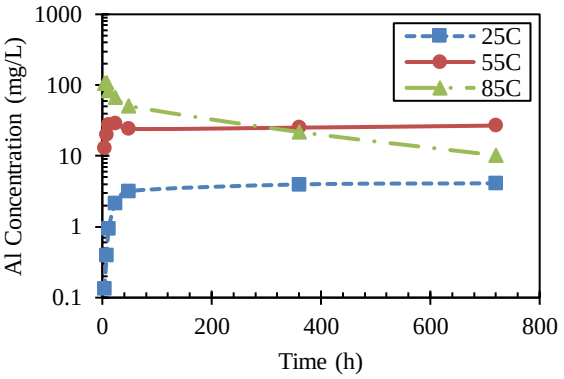

(b)

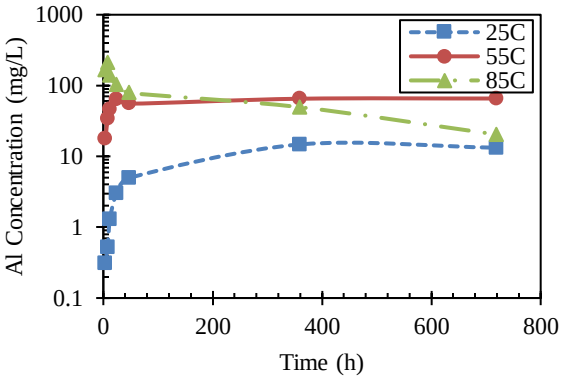

(c)

Figure 16: Concentration of Al over time of different borate buffer solution (a) pH 7.5 (b) pH 7.7 (c) pH 8.2

5.3 Relationship of temperature and pH on Al releasing

Figure 17 shows that temperature have little effect on Al releasing rate at 4 hours at lower temperatures, while at higher temperature, the releasing rate of Al increases tremendously. In comparison to 12 hours of Al exposure time, depicts that the trend was similar, however the gradient of the curve at lower temperature is now closer to the gradient of Al releasing rate at higher temperatures. There is a break in chain at 24 hours of Al exposure time, the Al releasing rate increases more as temperature increases at pH of 8.2. This is possible caused by the dissolution of oxide layer in the first 24 hours. This is also proved by the amount of releasing rate in the first 24 hours were significantly higher than the release rate of Al after 24 hours. Therefore, from this results shows the importance of the effect of temperature and pH at the first 24 hours are most significant. As the trend continues to 30 days, the effect of temperature and pH lessens on Al releasing rate lessens. As shown in Figure 17 (f), the releasing rate of Al dropped at higher temperature environment. This may also be a caused by the buildup of Al oxide layer on the surface of the coupon after 30 days.

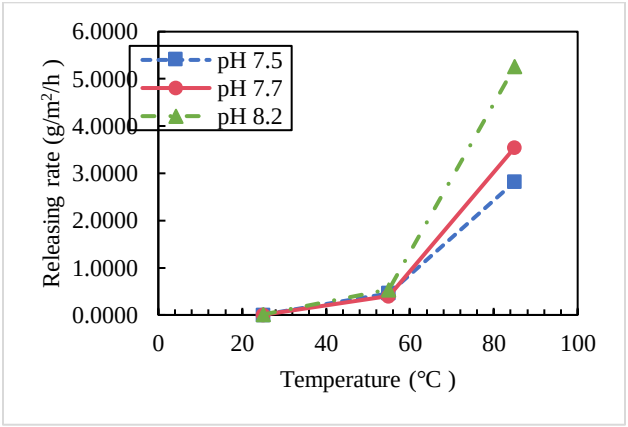

(a)

(b)

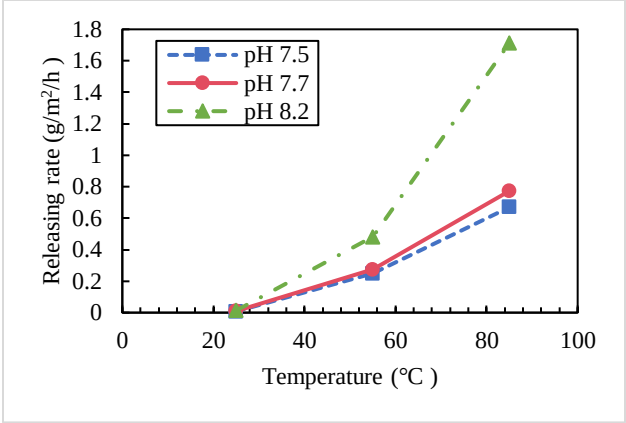
pH 7.5
pH 7.7
pH 8.2
Releasing rate (g/m²/h)
Temperature (℃)
0
0.2
0.4
0.6
0.8
1
1.2
1.4
1.6
1.8
0
20
40
60
80
100

(c)

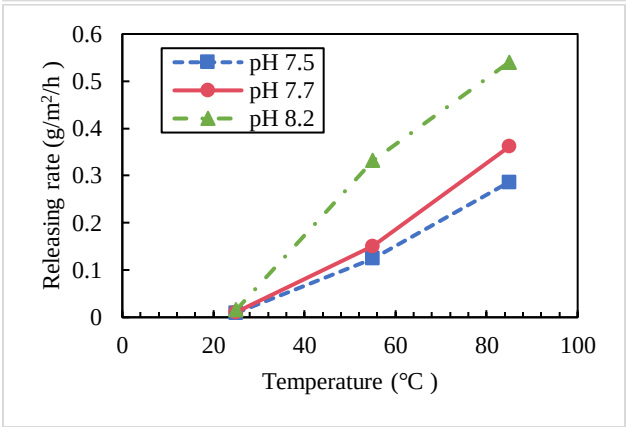
pH 7.5
pH 7.7
pH 8.2
Releasing rate (g/m²/h)
Temperature (℃)
0
0.1
0.2
0.3
0.4
0.5
0.6
0
20
40
60
80
100

(d)

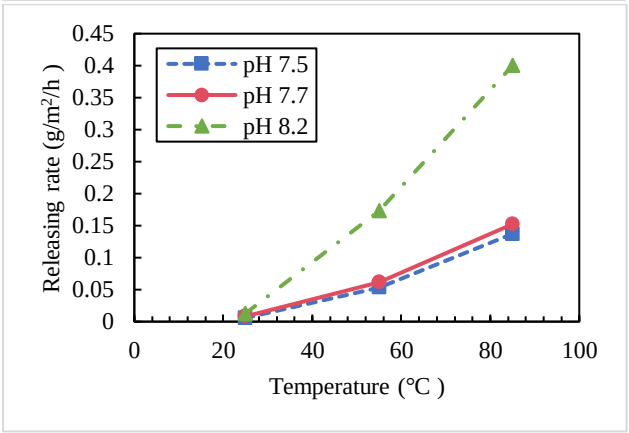
pH 7.5
pH 7.7
pH 8.2
Releasing rate (g/m²/h)
Temperature (℃)
0
0.05
0.1
0.15
0.2
0.25
0.3
0.35
0.4
0.45
0
20
40
60
80
100

(e)

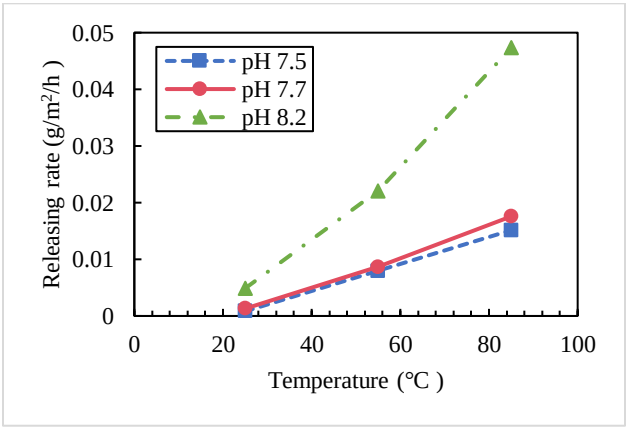
pH 7.5
pH 7.7
pH 8.2
Releasing rate (g/m²/h)
Temperature (℃)
0
0.01
0.02
0.03
0.04
0.05
0
20
40
60
80
100

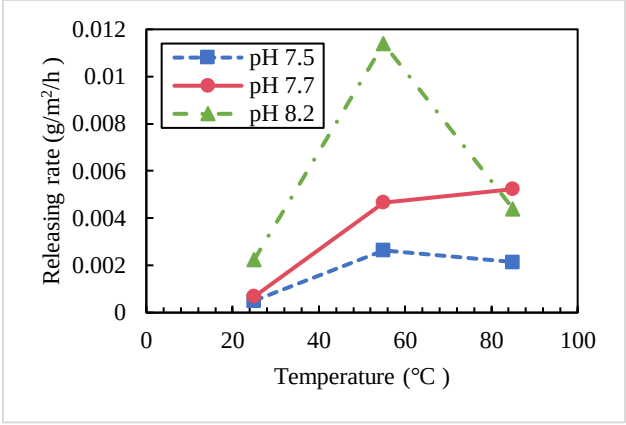

(f)

Figure 17: Releasing Rate of Al with temperature at (a) 8 hours (b) 12 hours (c) 24 hours (d) 48 hours (e) 360 hours (f) 720 hours

5.4 Relationship of Al Corrosion and Release Rate

Al release takes two forms; it is released into solution and it forms a scale layer on the material itself. Therefore, to get the whole picture of Al corrosion, both the Al content in the solution, and on the material coupon itself should be considered. As the Al is inserted into the bottle, corroded Al will precipitate into the solution, and this concentration of Al will be measured using ICP measurements. While the scale formed on the coupon will be descaled as described above to obtain the actual weight of the Al sample. From there, the actual corroded Al can be obtained. The amount of Al corroded can be determined based on the following equation [4].

$$Al_{corroded} = Al_{Released} + Al_{scale} \qquad \text{Equation 3}$$

where

$Al_{corroded}$ = Mass difference of Al coupon before and after cleaning

$Al_{released}$ = Mass of Al that leaves the coupon and enters the solution during the test, measured by ICP

Al_{scale} = Mass of Al that adheres to the coupon as scale layer

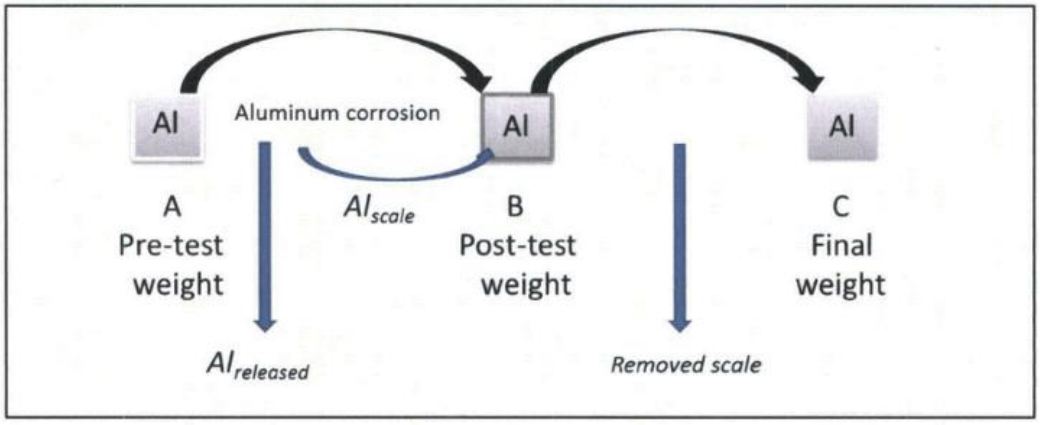

Figure 18: Measured weight of Al coupon to determine corrosion [4].

After the test, the decrease in mass of the Al sample represents that the Al was released in the solution or the original Al hydroxide layer was released. However, the release contains soluble and insoluble Al, and this cannot be differentiated through ICP. Therefore, the following equation is important to determine the actual corrosion rate of the Al New scale may also form on the surface of the sample, and this will add weight towards the coupon. Therefore, to include the mass of the corrode Al that adhered to the scale layer required measuring the mass of Al at the end of the test.

$$CR = \frac{M}{A_s \times t} \qquad \text{Equation 4}$$

where

$CR = \text{Corrosion Rate } \left[\frac{\text{g}}{\text{m}^2 \cdot \text{hrs}}\right]$

$M = \text{Total Mass Lost [g]}$

$A_s = \text{Surface Area } [\text{m}^2]$

$t = \text{time of immersion in test solution (hrs)}$

$⌈A_s \times t⌉$ Equation *4*, normalized to the individual tested solution volume as well as measured surface area exposure of Al.

5.5 Effect of pH on Al corrosion over time

Based on Figure 19, the corrosion rate of Al showed similar traits across pH 7.5, 7.7 and 8.2. The corrosion rate of Al was the highest at 85 °C as seen. The corrosion of Al at 25 °C, 55 °C and 85 °C increases in a magnitude of 10. While the trend of the curve continuously decreases as the time of submersion of Al increases. The difference in a 10 times magnitude of corrosion rate between pH 7.5, 7.7 and 8.2 may be influenced by the dissolution of Al in a high pH 8.2 alkaline solution, this supports the claim from the Westinghouse report where at higher pH significantly increases the corrosion rate of Al. Results from Mitchell also shown similar trends of significant increase in corrosion rate at higher pH [4]. At 25 °C, the corrosion rate at pH 7.5 experience a drop between 8 hours to 12 hours, therefore the corrosion rate of Al will experience a reduction after 12 hours. Similarly, at 25 °C, the corrosion rate at pH 7.7 significantly drop at 4 hours to 8 hours, therefore this represents that the Al corrosion rate will reduce after 8 hours of contact with the coolant. At a pH level of 8.2, the trend of corrosion rate of Al linearly decreases as the time of contact with Al increases. This downward trend supports the reason that the dissolution of Al reduces as the formation of Al oxide layer increases.

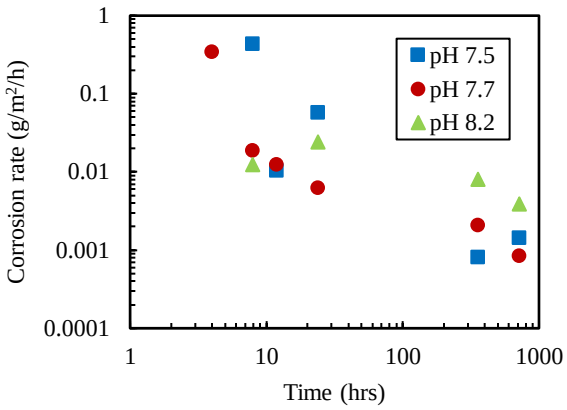

(a)

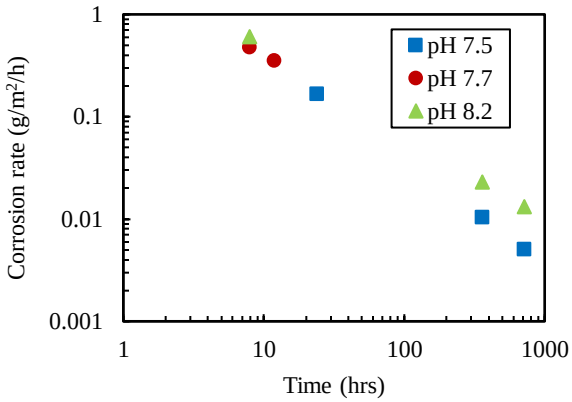

(b)

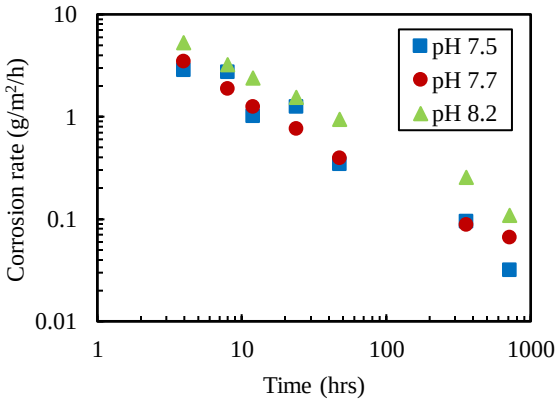

(c)

Figure 19: Corrosion Rate of Al over time at (a) 25 ℃ (b) 55 ℃ (c) 85 ℃

Based on Figure 20, the overall Al corrosion rate decreases as the temperature decreases, which corresponds to the trend of Al. releasing rate as discussed before. The corrosion rate of Al includes the formation of scale which is also known as a formation of oxide layer on the Al

sample and the release rate of Al. At the same time during the exposure of Al in the coolant environment, the Al behaviors has shown that over the period of first 24 hours the corrosion rate of Al is significantly higher, which is affected by the initial dissolution of Al layer.

The effect of pH on the corrosion rate of Al was seen to be the higher at higher pH buffer solutions, corresponding to a simulating of larger pipe break, the results showed similar trends of predict results from the WCAP prediction, whereby the corrosion rate of Al decreases proportionally with the inverse of absolute temperature [5].

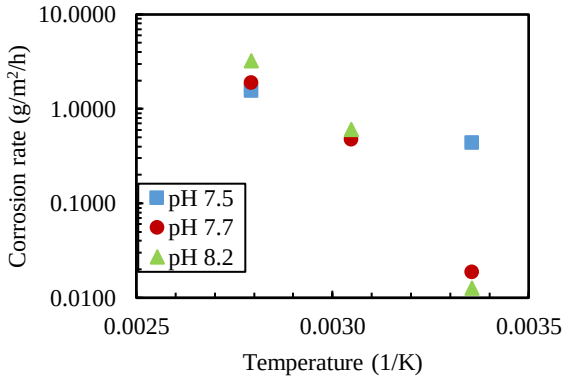

(a)

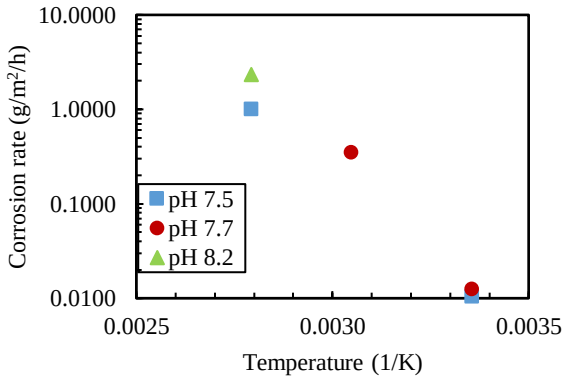

(b)

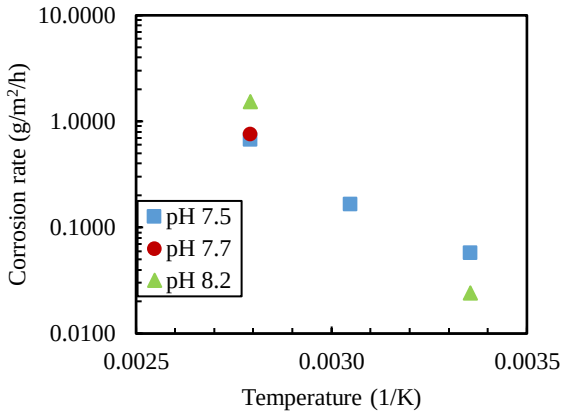
10.0000
1.0000
0.1000
0.0100
Corrosion rate (g/m²/h)
pH 7.5
pH 7.7
pH 8.2
0.0025
0.0030
0.0035
Temperature (1/K)

(c)

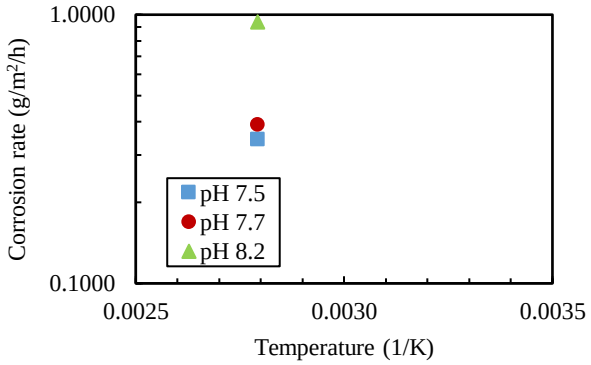
1.0000
0.1000
Corrosion rate (g/m²/h)
pH 7.5
pH 7.7
pH 8.2
0.0025
0.0030
0.0035
Temperature (1/K)

(d)

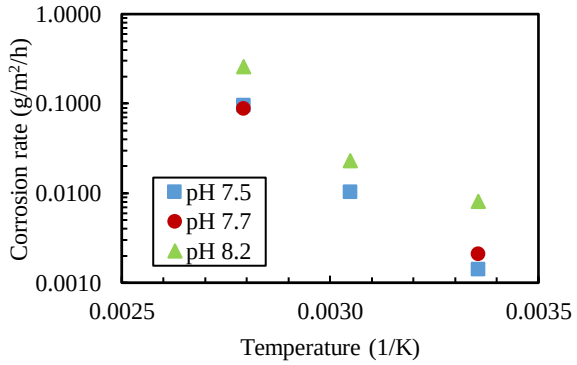
1.0000
0.1000
0.0100
0.0010
Corrosion rate (g/m²/h)
pH 7.5
pH 7.7
pH 8.2
0.0025
0.0030
0.0035
Temperature (1/K)

(e)

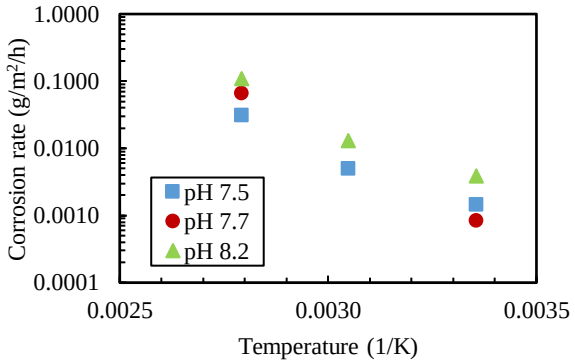

(f)

Figure 20: Corrosion Rate of Al at (a) 8 hours (b) 12 hours (c) 24 hours (d) 48 hours (e) 360 hours (f) 720 hours

Chapter 6: Summaries and Conclusions

The effect of temperature, pH value of borated alkaline solution and time of submersion on Al corrosion rate has been reviewed. Results show that an increase in temperature, increases the corrosion rate of Al as the submersion time of Al is longer. Similarly, the corrosion rate of Al increases as the pH value of the borated alkaline solution increases. There is also a significant increase in the amount of aluminum concentration between pH at 8.2 compared to the other solution at a lower pH. The main difference in the chemical composition of the solution is the presence of NaOH. The Al concentration is under a strong influence of high alkaline solution for the first 48 hours. At a temperature of 55 ℃, the Al concentration remains similar after 48 hours. Thus, the dissolution of Al is under the highest influence by the temperature at 55 ℃ before 48 hours. This is the same for 25℃ with pH 7.5 and 7.7, however at 8.2 the Al concentration continually increase. At this temperature, it has little influence on the releasing rate of the Al as the difference between releasing rate was small.

Results have shown that high temperature has little influence on the releasing rate of Al at 30 days. Dissolution of Al is closely related to the releasing rate of Al; results show that at 30 days, the solution and Al interaction, the releasing rate is lower at 85 ℃ compared to 55 ℃. The pH has the strongest effect on Al concentration in the first 48 hours of the solution and metal interaction. The reaction rate is slower than the transport rate after 48 hours.

The corrosion rate of Al decreases over time between pH 7.5 to 8.2. The corrosion rate at pH 8.2 experiences highest corrosion rate compared to pH 7.5 and 7.7. The difference of corrosion rate is minute at pH 7.5 and 7.7 due to the small change in pH.

References

[1] NRC, "Function of the Containment Sump," NRC, 13 May 2013. [Online]. Available: https://www.nrc.gov/reactors/operating/ops-experience/pwr-sump-performance/function-containment-sump.html.

[2] United States Nuclear Regulatory Commision, *Potential for Loss of Post-LOCA Recirculation Capability Due to Insulation Debris Blockage (Generic Letter No. 85-22)*, Washington D.C.: Uniter States Nuclear Regulatory Commision, 1985.

[3] C. B. Bahn, "CHEMICAL EFFECTS ON PWR SUMP STRAINER BLOCKAGE AFTER A LOSS-OF-COOLANT ACCIDENT: REVIEW ON U.S. RESEARCH EFFORTS," *Nuclear Engineering and Technology,* vol. 45, no. 3, pp. 295-310, Jun 3014.

[4] L. Mitchell, "Results of Bench Tests to Assess Corrosion of Aluminum in STP Containment Conditions," 2014.

[5] W. A. Byers, R. J. Jacko, A. E. Lane, E. J. Lahoda and R. D. Reid, "Evaluation of Post-Accident Chemical Effecs in Containment Sump Fluids to Support GSI-191," Westinghouse Electric Company LCC, Pittsburgh, 2008.

[6] M. R. Tabrizi, S. B. Lyon, G. E. Thompson and J. M. Ferguson, "The Long-Term Corrosion of Aluminum in Alkaline Media," *Corrosion Science,* vol. 32, no. 7, pp. 733-742, 1991.

[7] S. I. Pyun and S. M. Moon, "Solid State Electrochem," vol. 4, pp. 267-272, 2000.

[8] J. R. Davis, ASM Specialty Handbook: Aluminum and Aluminum Alloys, ASM Internationals, 1993.

[9] W. Stumm and J. J. Morgan, Aquatic Chemistry: Chemical Equilibria and Rates in Natural Waters, New York: John Wiley & Sons, 1995.

[10] D. Chen, B. Letellier and J. K. Howe, "Corrosion of Aluminum in the aqueous chemical environment of a loss-of-coolant accident at a nuclear power plant," *Corrosion Science,* vol. 50, pp. 1046-1057, 27 November 2007.

[11] K. Lorking and J. E. O. Mayne, Applied Chem II, 1961, pp. 170-180.

[12] M. Deltombe and M. Pourbaix, "Corrosion," 1959, pp. 496t-500t.

[13] L. Snizhko, A. L. Yerokhin, N. Gurevina, D. Misnyankin, A. Pilkington, A. Leyland and A. Matthews, "A model for glavanostatic anodising of Al in alkaline solutions," *Electrochimica Acta,* vol. 50, pp. 5458-5464, 2005.

[14] D. Langmuir, Aqueous Environmental Geochemistry, Colorado: Pearson, 1997.

[15] Z. Jinsuo, M. Klasky and B. C. Letellier, "The aluminum chemistry and corrosion in alkaline solutions," *Journal of Nuclear Materials,* vol. 384, no. 2009, pp. 175-189, 10 November 2008.

[16] D. Chu and R. F. Savinell, "Electrochem," no. 36, p. 1631, 1991.

[17] C. Beyrouty, G. E. Van Scoyoc and J. Feldkamp, "Evidence Supporting Specific Adsorption of Boron on Synthetic Aluminum Hydroxides," *Soil Science Society of America Journal,* vol. 48, no. 2, pp. 284-287, 10 Oct 1983.

[18] C. F. Baes and R. E. Mesmer, Hydrolysis of Cations, Krieger Pub Co, 1986.

[19] C. Su and D. L. Suarez, "Coordination of Adsorbed Boron: A FTIR Spectroscopic Study," *Environmental Science and Technology* , vol. 29, no. 2, pp. 302-311, 1995.

[20] T. Lavonen, "CHemical effects in the sump water pool during post-LOCA conditions," VVT Technical Research Center of Finland, 2013.

[21] R. E. Wolf, "What is ICP-MS?... and more importantly, what can it do?," USGS, March 2005. [Online]. Available: crustal.usgs.gov.

[22] A. Y. Musa, A. B. Mohamad, A. A. H. Kadhum and Y. B. A. Tabal, "Inhibition of Aluminum Alloy Corrosion in 0.5 M Nitric Acid Solution by 4-4-Dimethyloxazolidine-2-thione," *ASM International,* vol. 20, pp. 394-398, 2011.

[23] "Standard practice for preparing, cleaning, and evaluating corrosion test specimens," ASTM International, West Conshohocken, PA, 2011.

[24] M. Klasky, J. Zhang, M. Ding, B. Letellier, D. Chen and K. Howe, "Aluminum Chemistry in a Prototypical Post-Loss-of-a-Coolant-Accident, Pressurized Water Reactor Containment Environment," U.S. Nuclear Regulatory Commission, 2006.

[25] E. Lahti, J. Leavitt and J. Zhang, "Material Corrosion in a reactor containment sump following a loss-of-coolant accident," pp. 1-9, 3 March 2014.

[26] S. Guo, J. J. Leavitt, X. Zhou, E. Lahti and J. Zhang, "Corrosion of Aluminum alloy 1100 in post-LOCA solutions of a nuclear reactor," *Royal Society of Chemistry*, vol. 6, no. 2016, pp. 44119-44128, 27 April 2016.

[27] C. B. Bahn, K. E. Kasza and W. J. Shack, "Technical Letter Report on Follow-on Studies in Chemical Effects Head-Loss Research; Studies on WCAP Surrogates and Sodium Tetraborate Solutions," U.S. Nuclear Regulatory Commision, 2007.

Appendix

The following tables depicts the average raw data obtained in the experiments:

Table 2: Releasing Rate of Al at 85 ℃

Time (hrs)	Releasing rate (g/m^2/h)		
	pH 7.5	pH 7.7	pH 8.2
4	2.67E+00	3.28E+00	5.20E+00
8	1.36E+00	1.70E+00	3.29E+00
12	6.27E-01	8.61E-01	1.47E+00
24	2.34E-01	3.54E-01	5.33E-01
48	8.81E-02	1.32E-01	2.05E-01
360	4.82E-03	7.34E-03	1.63E-02
720	1.17E-03	1.68E-03	3.06E-03

Table 3: Al concentration at 85 ℃

Time (hrs)	Aluminum Concentration (mg/L)		
	pH 7.5	pH 7.7	pH 8.2
4	85.56	105.1	166.4
8	87.19	109.0	211.0
12	60.22	82.73	141.0
24	44.83	67.95	102.2
48	33.86	50.94	78.99
360	14.65	21.80	49.49
720	8.988	10.21	20.32

Table 4: Releasing Rate of Al at 55 ℃

Time (hrs)	Releasing rate (g/m^2/h)		
	pH 7.5	pH 7.7	pH 8.2
4	4.60E-01	4.00E-01	5.39E-01
8	3.52E-01	3.02E-01	5.29E-01
12	2.48E-01	2.74E-01	4.81E-01
24	1.24E-01	1.51E-01	3.32E-01
48	5.30E-02	6.30E-02	1.45E-01
360	7.98E-03	8.67E-03	2.21E-02
720	3.95E-03	4.66E-03	1.14E-02

Table 5: Al concentration at 55 ℃

Time (hrs)	Aluminum Concentration (mg/L)		
	pH 7.5	pH 7.7	pH 8.2
4	14.99	12.91	17.91
8	22.88	20.00	34.36
12	24.31	27.42	46.42
24	24.57	29.20	63.90
48	20.39	24.17	55.52
360	23.54	25.14	65.18
720	22.77	26.86	65.63

Table 6: Releasing Rate of Al at 25℃

Time (hrs)	Releasing rate (g/m^2/h)		
	pH 7.5	pH 7.7	pH 8.2
4	5.94E-03	4.22E-03	9.69E-03
8	6.01E-03	6.24E-03	8.11E-03
12	7.70E-03	9.89E-03	1.33E-02
24	9.26E-03	1.11E-02	1.56E-02
48	5.83E-03	7.67E-03	1.32E-02
360	8.25E-04	1.32E-03	4.87E-03
720	5.07E-04	6.78E-04	2.24E-03

Table 7: Al concentration at 25 ℃

Time (hrs)	Aluminum Concentration (mg/L)		
	pH 7.5	pH 7.7	pH 8.2
4	0.190	0.135	0.310
8	0.385	0.395	0.520
12	0.740	0.950	1.280
24	1.775	2.125	2.985
48	2.235	3.188	4.980
360	2.500	3.963	14.76
720	2.952	4.117	13.25

Table 8: Releasing Rate of Al at pH 7.5

Time (hrs)	Releasing rate ($g/m^2/h$)		
	25 ℃	55 ℃	85 ℃
4	5.94E-03	4.60E-01	2.67E+00
8	6.01E-03	3.52E-01	1.36E+00
12	7.70E-03	2.48E-01	6.27E-01
24	9.26E-03	1.24E-01	2.34E-01
48	5.83E-03	5.30E-02	8.81E-02
360	8.25E-04	7.98E-03	4.82E-03
720	5.07E-04	3.95E-03	1.17E-03

Table 9: Al Concentration at pH 7.5

Time (hrs)	Aluminum Concentration (mg/L)		
	25 ℃	55 ℃	85 ℃
4	0.190	14.99	85.56
8	0.385	22.88	87.19
12	0.740	24.31	60.22
24	1.775	24.57	44.83
48	2.235	20.39	33.86
360	2.500	23.54	14.65
720	2.952	22.77	8.988

Table 10: Releasing Rate of Al at pH 7.7

Time (hrs)	Releasing rate (g/m^2/h)		
	25 ℃	55 ℃	85 ℃
4	4.22E-03	4.00E-01	5.20E+00
8	6.24E-03	3.02E-01	3.29E+00
12	9.89E-03	2.74E-01	1.47E+00
24	1.11E-02	1.51E-01	5.33E-01
48	7.67E-03	6.30E-02	2.05E-01
360	1.32E-03	8.67E-03	1.63E-02
720	6.78E-04	4.66E-03	3.06E-03

Table 11: Al Concentration at pH 7.7

Time (hrs)	Aluminum Concentration (mg/L)		
	25 ℃	55 ℃	85 ℃
4	0.135	12.91	105.1
8	0.395	20.00	109.0
12	0.950	27.42	82.73
24	2.125	29.20	67.95
48	3.188	24.17	50.94
360	3.963	25.14	21.80
720	4.117	26.86	10.21

Table 12: Releasing Rate of Al at pH 8.2

Time (hrs)	Releasing rate (g/m^2/h)		
	25 ℃	55 ℃	85 ℃
4	9.69E-03	5.39E-01	5.20E+00
8	8.11E-03	5.29E-01	3.29E+00
12	1.33E-02	4.81E-01	1.47E+00
24	1.56E-02	3.32E-01	5.33E-01
48	1.32E-02	1.45E-01	2.05E-01
360	4.87E-03	2.21E-02	1.63E-02
720	2.24E-03	1.14E-02	3.06E-03

Table 13: Al Concentration at pH 8.2

Time (hrs)	Aluminum Concentration (mg/L)		
	25 ℃	55 ℃	85 ℃
4	0.310	17.91	166.4
8	0.520	34.36	211.0
12	1.280	46.42	141.0
24	2.985	63.90	102.2
48	4.980	55.52	78.99
360	14.76	65.18	49.49
720	13.25	65.63	20.32

Table 14: Releasing Rate of Al at 4 hours

pH	Temperature (℃)	Releasing Rate ($g/m^2/h$)
7.5	25	0.0059
	55	0.4605
	85	2.8206
7.7	25	0.0042
	55	0.4002
	85	3.5470
8.2	25	0.0097
	55	0.5395
	85	5.2615

Table 15: Releasing Rate of Al at 12 hours

pH	Temperature (℃)	Releasing Rate ($g/m^2/h$)
7.5	25	0.0077
	55	0.2483
	85	0.6692
7.7	25	0.0099
	55	0.2742
	85	0.7728
8.2	25	0.0133
	55	0.4813
	85	1.7127

Table 16: Releasing Rate of Al at 24 hours

pH	Temperature (℃)	Releasing Rate ($g/m^2/h$)
7.5	25	0.0093
	55	0.1245
	85	0.2866
7.7	25	0.0111
	55	0.1509
	85	0.3616
8.2	25	0.0156
	55	0.3318
	85	0.5406

Table 17: Releasing Rate of Al at 48 hours

pH	Temperature (℃)	Releasing Rate ($g/m^2/h$)
7.5	25	0.0058
	55	0.0533
	85	0.1372
7.7	25	0.0083
	55	0.0615
	85	0.1523
8.2	25	0.0130
	55	0.1729
	85	0.4001

Table 18: Releasing Rate of Al at 360 hours

pH	Temperature (℃)	Releasing Rate ($g/m^2/h$)
7.5	25	0.0008
	55	0.0080
	85	0.0151
7.7	25	0.0013
	55	0.0087
	85	0.0176
8.2	25	0.0049
	55	0.0221
	85	0.0473

Table 19: Releasing Rate of Al at 720 hours

pH	Temperature (℃)	Releasing Rate ($g/m^2/h$)
7.5	25	0.0005
	55	0.0026
	85	0.0021
7.7	25	0.0007
	55	0.0047
	85	0.0052
8.2	25	0.0022
	55	0.0114
	85	0.0044

Table 20: Corrosion Rate of Al over time at 85 ℃

pH	Time (hrs)	Corrosion Rate
7.5	4	2.847
	8	2.734
	12	1.007
	24	1.236
	48	0.344
	360	0.095
	720	0.031
7.7	4	3.437
	8	1.875
	12	1.250
	24	0.756
	48	0.389
	360	0.088
	720	0.066
8.2	4	5.266
	8	3.216
	12	2.360
	24	1.529
	48	0.940
	360	0.255
	720	0.108

Table 21: Corrosion Rate and Release Rate of Al at 8 hours

Temperature (C)	pH	Temperature (1/K)	Corrosion Rate (g/m2/h)	Releasing Rate (g/m2/h)	Scale Formation Rate (g/m2/h)
25	7.5	0.0034	0.4375	0.0060	0.4315
85		0.0028	1.5608	1.4385	0.1222
25	7.7	0.0034	0.0188	0.0062	0.0125
55		0.0030	0.4711	0.3020	0.1691
85		0.0028	1.8750	1.6992	0.1758
25	8.2	0.0034	0.0125	0.0081	0.0044
55		0.0030	0.6037	0.5291	0.0746
85		0.0028	3.2161	3.1192	0.0968

Table 22: Corrosion Rate and Release Rate of Al at 12 hours

Temperature (C)	pH	Temperature (1/K)	Corrosion Rate (g/m2/h)	Releasing Rate (g/m2/h)	Scale Formation Rate (g/m2/h)
25	7.5	0.0034	0.0104	0.0077	0.0027
85		0.0028	1.0074	0.6692	0.3382
25	7.7	0.0034	0.0125	0.0099	0.0026
55		0.0030	0.3520	0.2742	0.0779
85	8.2	0.0028	2.3602	1.5901	0.7701

Table 23: Corrosion Rate and Release Rate of Al at 24 hours

Temperature (C)	pH	Temperature (1/K)	Corrosion Rate (g/m2/h)	Releasing Rate (g/m2/h)	Scale Formation Rate (g/m2/h)
25	7.5	0.0034	0.0573	0.0093	0.0480
55		0.0030	0.1662	0.1245	0.0417
85		0.0028	0.6771	0.2335	0.4436
85	7.7	0.0028	0.7555	0.3579	0.3976
25	8.2	0.0034	0.0240	0.0156	0.0084
85		0.0028	1.5291	0.5366	0.9924

Table 24: Corrosion Rate and Release Rate of Al at 48 hours

Temperature (C)	pH	Temperature (1/K)	Corrosion Rate (g/m2/h)	Releasing Rate (g/m2/h)	Scale Formation Rate (g/m2/h)
85	7.5	0.0028	0.3444	0.1471	0.1974
85	7.7	0.0028	0.3891	0.1550	0.2341
85	8.2	0.0028	0.9397	0.4016	0.5381

Table 25: Corrosion Rate and Release Rate of Al at 360 hours

Temperature (C)	pH	Temperature (1/K)	Corrosion Rate (g/m2/h)	Releasing Rate (g/m2/h)	Scale Formation Rate (g/m2/h)
25	7.5	0.0034	0.0014	0.0008	0.0006
55		0.0030	0.0103	0.0080	0.0023
85		0.0028	0.0948	0.0163	0.0785
25	7.7	0.0034	0.0021	0.0013	0.0008
85		0.0028	0.0878	0.0174	0.0703
25	8.2	0.0034	0.0081	0.0051	0.0030
55		0.0030	0.0229	0.0221	0.0008
85		0.0028	0.2550	0.0431	0.2119

Table 26: Corrosion Rate and Release Rate of Al at 720 hours

Temperature (C)	pH	Temperature (1/K)	Corrosion Rate (g/m2/h)	Releasing Rate (g/m2/h)	Scale Formation Rate (g/m2/h)
25	7.5	0.0034	0.0014	0.0005	0.0009
55		0.0030	0.0050	0.0040	0.0011
85		0.0028	0.0313	0.0021	0.0291
25	7.7	0.0034	0.0008	0.0007	0.0001
85		0.0028	0.0659	0.0065	0.0594
25	8.2	0.0034	0.0039	0.0023	0.0016
55		0.0030	0.0130	0.0114	0.0016
85		0.0028	0.1082	0.0046	0.1035

The following figures are individual graphs relating temperature and pH value with corrosion rate and Al concentration:

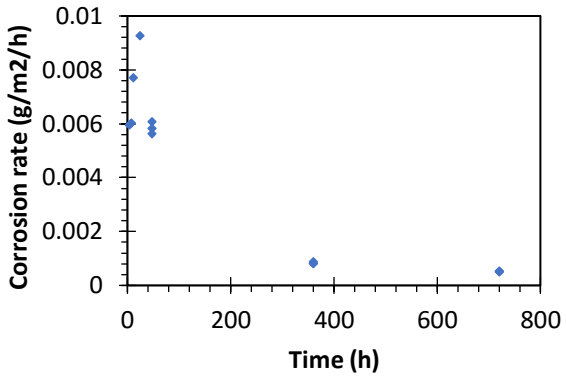

Figure 21: Corrosion Rate of Al pH 7.5 at 25 ℃

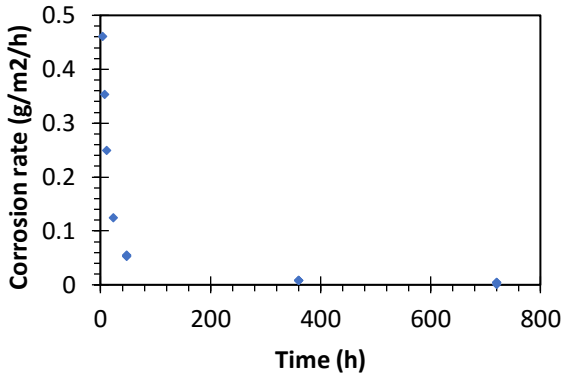

Figure 22: Corrosion Rate of Al pH 7.5 at 55 ℃

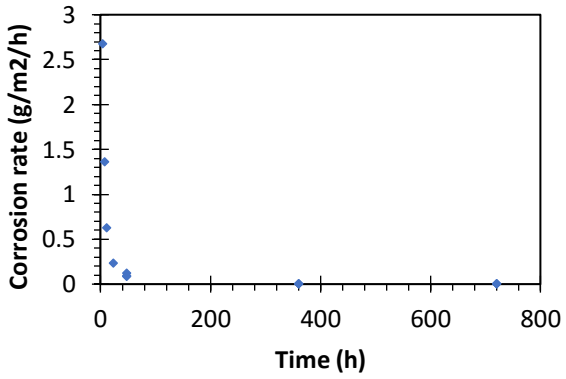

Figure 23: Corrosion Rate of Al pH 7.5 at 85 ℃

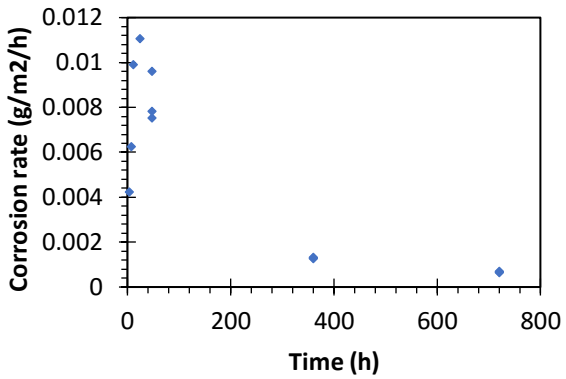

Figure 24: Corrosion Rate of Al pH 7.7 at 25 ℃

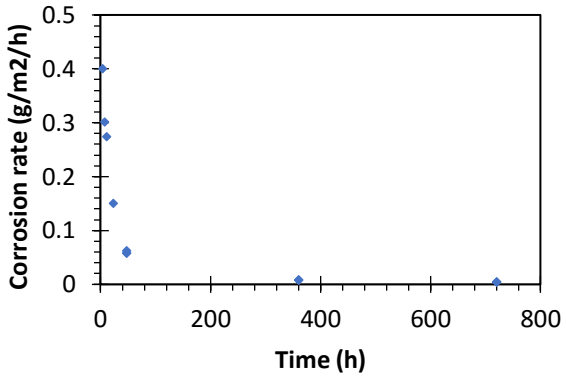

Figure 25: Corrosion Rate of Al pH 7.7 at 55 ℃

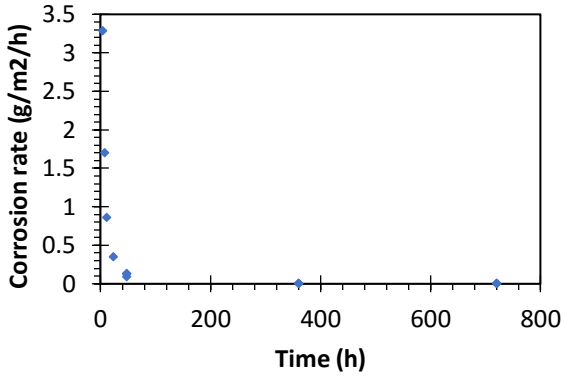

Figure 26: Corrosion Rate of Al pH 7.7 at 85 ℃

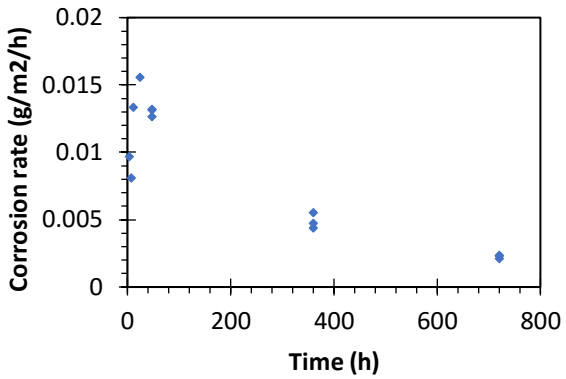

Figure 27: Corrosion Rate of Al pH 8.2 at 25 ℃

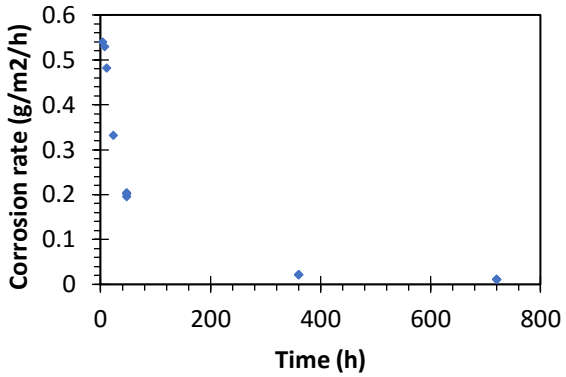

Figure 28: Corrosion Rate of Al pH 8.2 at 55 ℃

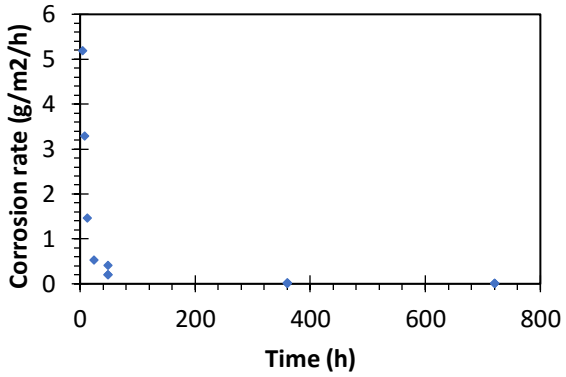

Figure 29: Corrosion Rate of Al pH 8.2 at 85 ℃